


REPORT DOCUMENTATION

AD-A238 615

Approved
L 0704-0188

Public reporting burden for this collection of information is estimated to average gathering and maintaining the data needed, and completing and reviewing the collection of information, including suggestions for reducing this burden, to Washington Headquarters, Suite 1204, Arlington, VA 22202-4302, and to the Office of Management and Administration, Suite 1204, Arlington, VA 22202-4302.

Using existing data sources,
for any other aspect of this
and Reports, 1215 Jefferson
Bl., DC 20543.

1. AGENCY USE ONLY (Leave blank)		2. REPORT DATE 18 JUL 1991		3. REPORT TYPE AND DATES COVERED ANNUAL 01 Dec 89 To 30 Nov 90	
4. TITLE AND SUBTITLE A SYSTEMS THEORETIC INVESTIGATION OF NEURONAL NETWORK PROPERTIES OF THE HIPPOCAMPAL FORMATION				5. FUNDING NUMBERS GR - AFOSR-89-0197 PE - 61102f PR - 2312 TA - A1	
6. AUTHOR(S) Theodore W. Berger				7. PERFORMING ORGANIZATION REPORT NUMBER AEOSR-TR- 91 0672	
7. PERFORMING ORGANIZATION NAME(S) AND ADDRESS(ES) University of Pittsburgh Department of Behavioral Neuroscience Pittsburgh PA 15206				8. PERFORMING ORGANIZATION REPORT NUMBER	
9. SPONSORING / MONITORING AGENCY NAME(S) AND ADDRESS(ES) Dr Haddad Air Force Office of Scientific Research Building 410 Bolling AFB DC 20332-6448 NL				10. SPONSORING / MONITORING AGENCY REPORT NUMBER	
11. SUPPLEMENTARY NOTES					
12a. DISTRIBUTION / AVAILABILITY STATEMENT Approved for public release; distribution unlimited				12b. DISTRIBUTION CODE A-1	
13. ABSTRACT (Maximum 200 words) The major emphasis during this past year of AFOSR support has been on refining the transputer network as a simulation tool. The structure of the functioning parallel computer system has been expanded to include all of the available transputer elements and the inter-processor communication pathways have been simplified and made more efficient. In addition, the user's interface has been refined to make the simulations a working tool for the experimentalist. Additional efforts were placed on minimizing computational errors inherent in the simulations and in investigating the accuracy of the simulations against alternative complex patterns of stimuli such as doublets and triplets. 91-05863 					
14. SUBJECT TERMS				15. NUMBER OF PAGES 20	
17. SECURITY CLASSIFICATION OF REPORT (U)				16. PRICE CODE	
18. SECURITY CLASSIFICATION OF THIS PAGE (U)		19. SECURITY CLASSIFICATION OF ABSTRACT (U)		20. LIMITATION OF ABSTRACT UNLIMITED	

**Best
Available
Copy**

The following Progress Report describes the results of the majority of our AFOSR-supported research for Year 2 of the project entitled "A Systems Theoretic Investigation of Neuronal Network Properties of the Hippocampal Formation." The Progress Report is divided into five sections: a brief overview of general experimental and analytical procedures; research characterizing nonlinear response properties of the *in vivo* dentate gyrus; the extension of this research to the *in vitro* hippocampal slice; computer simulations of nonlinear response properties of the dentate based on the experimental work; and a listing of publications during the past year of support.

GENERAL EXPERIMENTAL AND ANALYTICAL PROCEDURES

Preparations. All experiments are conducted using the hippocampus of male, New Zealand white rabbits. For experiments conducted both *in vivo* and *in vitro*, fibers of the perforant path were stimulated electrically and the evoked response of granule cells of the ipsilateral dentate gyrus were recorded from the cell body layer. Recordings of extracellular population spike and epsp responses are used to monitor global activity of populations of granule cells; intracellular recordings are used to monitor the activity of single neurons.

Random Impulse Train Stimulation. A random interval train of electrical impulses was used to stimulate perforant path fibers. The train consisted of a series of 4064 impulses with inter-impulse intervals drawn from a Poisson distribution. For most experiments conducted to date, the mean inter-event interval (λ) of the random train has been 500 ms and the range of inter-event intervals has been 1-5000 ms.

Analytical Procedures. Nonlinear input/output properties of the dentate are defined as the kernels of a functional power series expansion:

$$y(t) = G_0 + G_1[h_1, x(t)] + G_2[h_2, x(t)] + G_3[h_3, x(t)] + E \quad (1)$$

where $y(t)$ is the output of dentate granule cells, (G_i) is a set of mutually orthogonal functionals, (h_i) is a set of symmetric kernels which characterize the relationship between the input and output, and E is an error term due to truncation. The train of discrete input events defined by $x(t)$ is a set of δ -functions representing the stimulus train. The first four kernels of the series are obtained by the process of orthogonalization using cross-correlation techniques applied to point process events.

Interpretation of the Kernel Functions. The first order kernel, $h_1(\tau)$, is the average of all evoked dentate population spike responses (with a latency of τ) occurring during train stimulation. The second order kernel, $h_2(\tau, \Delta)$, represents the modulatory effect of a preceding stimulus occurring Δ ms earlier on the number of granule cells activated (with a latency of τ) by the most current stimulation impulse, irrespective of any other impulses which may occur during that interstimulus interval. The third order kernel, $h_3(\tau, \Delta_1, \Delta_2)$, represents the modulatory effect of any two preceding stimuli occurring Δ_1 ms and Δ_2 ms earlier on the number of granule cells activated by the most current stimulation impulse, irrespective of any other impulses which may occur during either interval. In a more general sense, the kernel functions provide a complete characterization of the functional properties resulting from the interaction among whatever system of neural elements is studied (the elements comprising the system may be conductances, single neurons, populations of neurons) studied

As a result, the kernels provide a basis for predicting the activity of those elements in response to any arbitrarily selected stimulus condition.

NONLINEAR SYSTEMS ANALYSIS of the *in vivo* HIPPOCAMPAL DENTATE GYRUS

In experiments conducted previously, we characterized nonlinear response properties of granule cells recorded *in vivo*. When a relatively low stimulus intensity was used for random impulse train stimulation (one that evoked a population spike amplitude approximately 10% of maximum when the perforant path was stimulated using single impulses delivered at 0.5 Hz), first order kernels showed that the average population spike amplitude was 2.2 ± 0.3 mV (Figure 1, upper panel).

Second order kernels indicated that granule cell output exhibited prominent nonlinearities in response to several ranges of interstimulus intervals: population spike amplitude was almost completely suppressed when preceding impulses occurred within 10-30 ms (Figure 1, middle panel), and there was a marked facilitation of spike amplitude when preceding impulses occurred within 50-400 ms. Maximum facilitation was exhibited when $\Delta=90-100$ ms. Intervals greater than 1000 ms induced no consistent change in spike amplitude.

Prominent third order nonlinearities were expressed when the intervals separating any pair of preceding intervals was $\leq 200-300$ ms. In response to these stimulus patterns, granule cell output was reduced by an average maximum of approximately 60% of the first order kernel. with the magnitude of suppression inversely related to interval length (Figure 1, bottom panel).

Nonlinear Response Properties of Hippocampal Dentate Granule Cells: Dual Input Stimulation of Medial Perforant Path and Commissural Afferents. One the major goals of the experiments conducted *in vivo* is to determine the contribution to the nonlinearities described above that is made by each major feedback and feedforward pathway connecting the dentate with other subsystems of the hippocampus. During this past year, we have investigated functional interactions between medial perforant path and commissural inputs to the hippocampal dentate gyrus using a dual input stimulation procedure. The medial perforant path first was stimulated alone with a random interval impulse train ($\lambda=2$ Hz). Random impulse train stimulation then was repeated with simultaneous stimulation of commissural afferents (contralateral hilus) using a constant frequency of 2.0 Hz.

Results showed that simultaneous stimulation of commissural input decreased the first order kernel (Figure 2, right panels), consistent with previous reports of an inhibitory effect of commissural afferents on medial perforant path input to granule cells. In addition, however, second order kernel facilitation for $\Delta=100-400$ ms was decreased markedly; second order kernel inhibition was reduced to a lesser degree, occurring in response to a smaller range of Δ s. Simultaneous stimulation of commissural afferents did not affect second order kernel values for any other Δ s. Third order nonlinearities were decreased in magnitude for all combinations of intervals. These results are the virtual complement of the effects of unilateral hippocampectomy: an increase in the first order kernel average, a small increase in second order inhibition, a substantial increase in second order facilitation, and an augmentation of the magnitude of third order nonlinearities (Figure 2, left panels). Thus, commissural feedback to the dentate does not appear to underlie granule cell nonlinearities in response to any particular interval or set of intervals. Instead, commissural feedback modulates the gain of nonlinearities expressed in response to other feedback pathways or intracellular mechanisms.

NMDA and Non-NMDA Receptor-Mediated Components of the Population EPSP Recorded *in vivo* from Hippocampal Dentate Granule Cells. During Year 1 of AFOSR support, we investigated the nonlinearities expressed in the population synaptic responses of granule cells, and found them to differ fundamentally from those expressed in population spike activity. We continued our analysis of the population EPSP during Year 2, and concentrated on developing procedures for pharmacological isolation of relative contribution of the two classes of glutamatergic receptor subtypes which mediate perforant path input to granule cells.

Previous studies of perforant path-evoked EPSPs of dentate granule cells have shown that, in response to low frequency (<0.2 Hz) stimulation, the NMDA receptor-mediated component is relatively small compared to the kainate/quisqualate receptor-mediated component. Thus, population EPSPs recorded *in vivo* are reported not to be reduced by the selective NMDA receptor antagonist D-APV. However, intracellular studies of the dentate *in vitro* have found that CNQX, an antagonist selective for kainate/quisqualate receptors eliminates all but a small D-APV sensitive portion of the granule cell EPSP. In an effort to define the optimal conditions for studying NMDA-mediated synaptic transmission *in vivo*, we examined population EPSPs recorded from the molecular layer of the rabbit dentate gyrus, while administering CNQX, D-APV, or saline by microinfusion through a multibarrelled pipette positioned 100-500 μm from the recording site.

CNQX (25-50 μM) reduced the evoked EPSP by 70-95% ($n=12$) without affecting the afferent fiber volley; however, in all cases tested ($n=8$), subsequent addition of D-APV (50-100 μM) substantially reduced the remaining response (Figure 3). For greater resolution of the component sensitive to D-APV, we used digital subtraction of responses evoked during the application of CNQX and D-APV from those evoked in the presence of CNQX alone. The residuals clearly revealed that D-APV eliminated a negative-going potential with a peak latency 25-200% longer than the control peak (10.0 ms vs 5.1 ms control) and a peak amplitude of up to 20% of the control amplitude. In separate experiments, D-APV was applied alone and evoked responses were subtracted from those recorded in the presence of saline. These remainders had a time course very similar to the CNQX-APV residuals. When responses were recorded simultaneously from the cell body and molecular layers, the D-APV sensitive components observed in the two laminae were of opposite polarity indicating that the NMDA-mediated response was generated locally. Parametric manipulations ($n=8$) indicated that the amplitude of this component is strongly frequency dependent, and is greatly enhanced (200% of the amplitude to a single impulse) in response to 2-5 impulses delivered with a 2 ms interstimulus interval. These results indicate that the NMDA-mediated component of perforant path input to dentate granule cells may be studied effectively *in vivo* in the presence of CNQX and with bursts of high frequency stimulation.

NMDA Receptor-Mediated Potentiation of Perforant Path Input to CA3 Hippocampal Pyramidal Cells. During Year 1 of AFOSR support, we described for the first time the electrophysiological characteristics of monosynaptic perforant path input to CA3 pyramidal neurons. Although dentate granule cell input to CA3 cells is glutamatergic, excitation transmitted through this pathway does not include a component mediated by NMDA receptors. NMDA receptors have been localized in the apical dendritic region of CA3 pyramidal neurons, however, including the subzone innervated by perforant path afferents. In a series of experiments, we evaluated the functional contribution of NMDA receptor-mediated input to CA3 cells using the specific antagonist, D-APV, in an attempt to block the induction of LTP in the perforant path projection.

Stimulating electrodes were placed in the ipsilateral angular bundle, the ipsilateral hilus, and the contralateral CA3 cell layer of halothane anesthetized rabbits. In one series of experiments, 10 trains of 10 impulses (400 Hz) were delivered to the angular bundle while recording simultaneously from the CA3 and dentate granule cell body layers. Analysis of input/output functions for monosynaptically evoked population spikes revealed that LTP was induced in CA3 pyramidal neurons and dentate granule cells (10/12 animals; >30 min). In the presence of the NMDA-receptor antagonist, D-APV (50-100 μ M; pressure-injected), LTP was not induced (8/8 animals) following perforant path tetanus. When lower concentrations of D-APV were used, LTP could be induced >90 min after drug application. In addition, LTP could be blocked selectively in either the dentate gyrus or CA3 with localized injections of D-APV (Figure 4).

The existence of monosynaptic input to CA3 pyramidal neurons is highly significant because our model of the hippocampus must be formulated as a feedforward pathway rather than as a cascade. The existence of a significant NMDA-mediated component of transmission through this pathway suggests that the feedforward connection could contribute significantly to nonlinearities in the input/output properties of CA3 pyramidal cells because of the prominent voltage-dependent blockade of the NMDA channel by Mg^{++} ions.

NONLINEAR SYSTEMS ANALYSIS of the *in vitro* HIPPOCAMPAL DENTATE GYRUS

We are making extensive use of the *in vitro* hippocampal slice as a preparation that eliminates virtually all feedback to the dentate from other subfields of the hippocampus, allowing an identification of granule cell response dynamics that originate from intrinsic mechanisms only. As we reported last year, nonlinearities expressed by granule cells *in vitro* are significantly different from those expressed by the same cell population *in vivo*. For example, second order nonlinearities of the *in vitro* slice (Figure 5, middle panel) were equally prominent, but were qualitatively different than those exhibited by *in vivo* preparations. Instead of suppression of granule cell output in response to short inter-impulse intervals, a robust facilitation was observed. The facilitation was greater in magnitude (with respect to normalized kernel values, $241 \pm 27\%$), occurred maximally in response to shorter intervals (10-20 ms) compared to data from *in vivo* preparations, and was expressed only in response to intervals less than 100-150 ms, a much narrower range than observed *in vivo*. In addition, data from slices consistently exhibited suppression to intervals of 150-800 ms; interstimulus intervals within the same range produced facilitation or no effect for *in vivo* preparations.

Third order kernels from slices revealed suppression of a larger magnitude (normalized values, average maximum of 90%), and in response to a much narrower range of intervals (<90 ms) than was observed for the *in vivo* dentate gyrus (Figure 5, lower panel). Third order nonlinearities for *in vitro* slices also included a robust facilitation in response to input patterns defined approximately by $\Delta_1=100-200$ ms and $\Delta_2=300-400$ ms, which was not observed *in vivo*.

Open-Loop Characteristics of Dentate Granule Cells. During the past year, we have attempted to achieve an open-loop condition for granule cells by experimentally eliminating any feedback or feedforward connections with interneurons with the dentate. Two specific experimental protocols have been developed to eliminate the possibility that other cell populations may contribute to *in vitro* granule cell input/output properties during stimulation of the perforant path. The first protocol involved physically separating a portion of the dentate gyrus from the rest of the slice preparation to

ensure that the other main cell layers of the hippocampus (i.e., CA1 and CA3) were not influencing granule cell responses. The separation procedure results in a reduced slice preparation that contains about half of the dentate gyrus (both cell body and molecular layers), a small portion of the hilus close to the granule cell body layer and the hippocampal fissure where perforant path fibers enter the dentate molecular layer. When population spike amplitudes were compared before and after the separation protocol (Figure 6), average second order kernels revealed no significant changes in the nonlinear response properties of the remaining population of granule cells. And like the intact slices, when exposed to the GABA_A antagonist bicuculline methiodide (10 μ M), the "reduced" slice preparations showed an increase in the facilitation observed for intervals of 10-100 ms.

In addition to dentate isolation, we also have sought to reduce the influence of other cell populations by decreasing the thickness of slices, from 600 μ m to 300 μ m. Some interneuron populations, most notably GABAergic interneurons, are thought to project parallel to the longitudinal axis of the hippocampus (and thus perpendicular to the plane of section of transverse slices). By decreasing the thickness of transverse slices, the influence of these cell populations should be reduced. To determine whether the influence of GABAergic interneurons was affected, the nonlinear response properties of granule cells were examined for both 600 and 300 μ m slices in the absence and presence of bicuculline methiodide (10 μ M). As demonstrated in Figure 7, bicuculline had the expected effect on granule cell population spike amplitude in 600 μ m slices (i.e., an increase in facilitation for intervals of 10-100 ms), whereas there was no significant effect of bicuculline on the second order response properties of granule cells in 300 μ m slices, thus suggesting that the influence of GABAergic interneurons had been eliminated in the thinner slices. Further studies are now in progress to determine the contribution of other population of interneurons within the hilus to the nonlinear response properties of granule cells and eliminate these influences where possible. In addition, further paired intra- and extracellular recordings will be performed in slice preparations which represent optimal open-loop conditions for granule cells.

Comparison of Single and Population Granule Cell Response Properties. To better evaluate nonlinearities expressed at the single cell level, we simultaneously recording intracellular membrane potentials and extracellular field potentials from electrodes that were less than 300 μ m apart in the cell body layer of the dentate gyrus during stimulation of perforant path fibers with a random impulse train. The intensity of stimulation, as determined by stimulus/response functions, was 10-30% of the intensity which elicited the maximum population spike response. Thus far, simultaneous recordings have been obtained from 16 single cell/population response pairs. Figure 8 illustrates average first, second and third order kernels for 7 preparations which received all 4064 impulses in the random impulse train. The average first order kernel for extracellular responses was 0.40 ± 0.16 mV, and the average first order kernel for single cells was 46%. Average second order kernel revealed that the nonlinear response properties associated with single granule cells were consistent with the nonlinear response properties of populations of granule cells. Specifically, both the probability of single cell discharge and the amplitude of population spikes were increased when the interstimulus interval between a pair of stimuli was 10-100 ms, with maximum facilitation occurring for interimpulse intervals of less than 20 ms. Single cell discharge and population spike amplitude were suppressed to a moderate degree when intervals were 150-600 ms.

Average third order kernels also revealed similarities in the nonlinear response properties of single granule cells and populations of granule cells. When two preceding intervals were both less than 150 ms, the probability of single cell discharge and population spike amplitude were less than

first order kernel values. Maximum suppression occurred when both intervals were less than 60 ms. Input resistance was not significantly affected by the random train stimulation.

Effects of Enhancing GABA_A Receptor-Mediated IPSPs on Nonlinear Response Properties of Dentate Granule Cells. We have previously shown that the response of granule cells to perforant path stimulation in the slice is characterized by facilitation of population spike amplitude when ISIs are 10-50 ms. In contrast, in the intact animal, suppression of spike amplitude is observed for the same ISIs. Our working hypothesis has been that this difference in nonlinear properties between the *in vitro* and the *in vivo* preparations is due to a decreased GABAergic inhibition in the slice. Supporting this hypothesis are results from experiments in which the GABA_A allosteric agonist alphaxalone has been shown to induce selectively a decrease in population spike amplitude for ISIs <100 ms.

During the past year we used intracellular recordings techniques to further characterize the actions of alphaxalone on the dentate gyrus. Specifically, the goal of these experiments was to determine: (1) the pharmacological effects of alphaxalone on membrane properties of dentate granule cells; (2) the dose-response characteristics of the alphaxalone-induced increase in IPSP efficacy; and (3) if the exposure to alphaxalone changes second order nonlinearities in a manner similar to that shown previously for the extracellular population spike.

We found that at all concentrations used (0.3, 3.0 and 30 μ M) alphaxalone decreased the input resistance of granule cells in a dose dependent manner ($-1.6 \pm 3.1\%$, $n=9$; $-12 \pm 1.4\%$, $n=11$; and $-21.2 \pm 1.8\%$, $n=8$, respectively; Figure 9). We also found that alphaxalone increased the amplitude of IPSPs elicited orthodromically, without significantly changing reversal potentials (Figure 10). These effects were blocked by GABA_A antagonist, bicuculline, indicating the receptor specificity of alphaxalone's effects.

As with changes in input resistance, the effects of alphaxalone on IPSP amplitude were dose-dependent: 0.3 μ M had inconsistent effects on most of granule cell properties observed; 3.0 μ M enhanced amplitude of the fast IPSP in the slice preparation close to the level observed *in vivo*; 30 μ M further enhanced the fast IPSP and suppressed the EPSP dramatically, so that no orthodromic action potential could be induced even with maximum stimulation intensity.

As demonstrated by second order kernel calculations (Figure 11), alphaxalone (3.0 μ M) had the expected effect of reversing the facilitation of the single cell spike probability in response to interstimulus intervals of 10-100 ms. Thus, based on the time course of the fast IPSP and the effects of alphaxalone on granule cell synaptic responses, the effect of alphaxalone on granule cell second order nonlinearities is most likely due to an enhancement of GABA_A-mediated IPSPs and a resulting decrease in the probability of action potential generation. The alphaxalone-induced change in second order nonlinearities of probability in single cell discharge is consistent with our previous finding using amplitude of population spike response.

THEORETICAL STUDIES AND COMPUTER SIMULATIONS

The major emphasis during this past year of AFOSR support has been on refining the transputer network as a simulation tool. The structure of the functioning parallel computer system has been expanded to include all of the available transputer elements and the inter-processor

communication pathways have been simplified and made more efficient. In addition, the user's interface has been refined to make the simulations a working tool for the experimentalist. Additional efforts were placed on minimizing computational errors inherent in the simulations and in investigating the accuracy of the simulations against alternative complex patterns of stimuli such as doublets and triplets.

One of the other major efforts made during the past year was to more fully develop computational tools for higher order Laplace transforms of the experimentally determined kernels. In the hippocampal formation, however, there are elements which cannot be isolated and whose input/output elements must be inferred from their effect on the other directly observable groups of neurons. To accomplish this the n^{th} order Laplace transforms of the impulse responses must be computed and algebraically manipulated. Models of the observable and unobservable subsystems, as well as the entire system, may thus be computed in terms of n^{th} order convolution operators.

A particular case dealt with during this past year involved the following three preparations: the intact hippocampal formation, with the dentate granule cell layer considered as a feedforward element, and the remainder of the ipsilateral hippocampus as a feedback element; a partially closed-loop system, where the contralateral hippocampus has been removed; and an open-loop system, where the contralateral hippocampus has been removed, the ipsilateral trisynaptic pathway is open, and the local GABAergic pathways have been blocked. Three sets of results were determined: (1) the n^{th} order Laplace transforms for the kernels characterizing each preparation; (2) the results of the algebraic manipulation of the n^{th} order transforms were used to calculate the unobservable elements, which in this case were GABAergic basket cells, and (3) the results of simulations used to verify the estimated kernels. The solutions allow computations of the kernels for the GABAergic pathway, which is available by direct measurement.

PUBLICATIONS DURING YEAR 2 OF AFOSR SUPPORT

Journals and Book Chapters:

Berger, T.W., Basset, J.L., and Orr, W.B. Multiple memory systems and their contribution to classical conditioning. In L. Dachowski and C. Flaherty (Eds.), Current Topics in Animal Learning: Brain, Emotion, and Cognition. N.Y.: Plenum, 1990, pp. 271-310.

Sclabassi, R.J., Krieger, D.N., Barrionuevo, G., Levitan, S.P., and Berger, T.W. Identification of hippocampal network function. Proceedings of the International Conference of the IEEE/EMBS, 1990, pp. 1886-1888.

Berger, T.W., Barrionuevo, G., Levitan, S.P., Krieger, D.N., and Sclabassi, R.J. Nonlinear systems analysis of network properties of the hippocampal formation. In J.W. Moore and M. Gabriel (Eds.), Neurocomputation and Learning: Foundations of Adaptive Networks. Cambridge, MA: MIT Press, 1991, pp. 283-352.

Robinson, G.B., Sclabassi, R.J., and Berger, T.W. Kindling-induced potentiation of excitatory and inhibitory inputs to hippocampal dentate granule cells. I. Effects on linear and nonlinear response characteristics. Brain Research, in press.

Berger, T.W., and Yeckel, M.F. Long-term potentiation of entorhinal afferents to the hippocampus: Enhanced propagation of activity through the trisynaptic pathway. In M. Baudry and J. Davis (Eds.), Long-Term Potentiation: A Debate of Current Issues. Cambridge, MA: MIT Press, in press.

Berger, T.W. and Basset, J.L. System properties of the hippocampus. In I. Gormezano (Ed.), Learning and Memory: The Biological Substrates. Hillsdale, N.J.: Lawrence Erlbaum, in press.

Manuscripts Submitted for Publication:

Balzer, J.R., Sclabassi, R.J., and Berger, T.W. Nonlinear systems analysis of medial perforant path input to the hippocampal dentate gyrus: Effects of stimulus intensity.

Harty, T.P., Berger, T.W., Sclabassi, R.J., and Barrionuevo, G. Nonlinear systems analysis of the *in vitro* hippocampal dentate gyrus. I. Characterization of granule cell response to perforant path input. Submitted for publication.

Harty, T.P., Berger, T.W., Sclabassi, R.J., and Barrionuevo, G. Nonlinear systems analysis of the *in vitro* hippocampal dentate gyrus. II. Contribution of GABA_A receptor function. Submitted for publication.

Krieger, D.N., Berger, T.W., and Sclabassi, R.J. Instantaneous characterization of time-varying nonlinear systems. Submitted for publication.

Published Abstracts:

Yeckel, M.F. and Berger, T.W. An *in vivo* comparison of the induction of long-term potentiation for perforant path, mossy fiber, and commissural input to CA3 pyramidal cells. Abstracts of the Fourth Conference on the Neurobiology of Memory, Irvine, CA, 1990.

Blanpied, T.A., Barrionuevo, G. and Berger, T.W. NMDA receptors mediated a component of granule cell responses to low frequency stimulation of perforant path afferents *in vivo*. Society for Neuroscience Abstracts, 1990, 16, p. 1184.

Xie, X., Harty, T.P., Scwabassi, R.J., Berger, T.W. and Barrionuevo, G. Alphasalone-enhanced alter nonlinearities of hippocampal dentate granule cells. Society for Neuroscience Abstracts, 1990, 16, p. 738.

Harty, T.P., Xie, X., Scwabassi, R.J., Berger, T.W. and Barrionuevo, G. Intracellular analysis of the nonlinear response properties of hippocampal dentate granule cells. Society for Neuroscience Abstracts, 1990, 16, p. 738.

Yeckel, M.F. and Berger, T.W. NMDA-dependent LTP of monosynaptic entorhinal input to CA3 and the dentate gyrus alters propagation of activity through the trisynaptic pathway. Society for Neuroscience Abstracts, 1990, 16, p. 491.

Berger, T.W., Weikart, C.L. and Scwabassi, R.J. Nonlinear response properties of hippocampal dentate granule cells: Dual input stimulation of medial perforant path and commissural afferents. Society for Neuroscience Abstracts, 1990, 16, p. 739.

Krieger, D., Berger, T.W., Weisz, D. and Scwabassi, R.J. Characterization of time-varying behavior in nonlinear systems. Society for Neuroscience Abstracts, 1990, 16, p. 738.

Scwabassi, R.J., Biedka, T., Solomon, J., Krieger, D., Barrionuevo, G. and Berger, T.W. Computation of unobserved hippocampal elements. Society for Neuroscience Abstracts, 1990, 16, p. 738.

Thiels, E., Weisz, D. and Berger, T.W. Reduction of activity of the glycine site at the NMDA receptor complex interferes with the induction of LTP *in vivo*. Society for Neuroscience Abstracts, 1990, 16, p. 1184.

Chauvet, G. and Berger, T.W. Two-level field theory interpretation of hippocampal extracellular field potentials. Society for Neuroscience Abstracts, 1990, 16, p. 739.

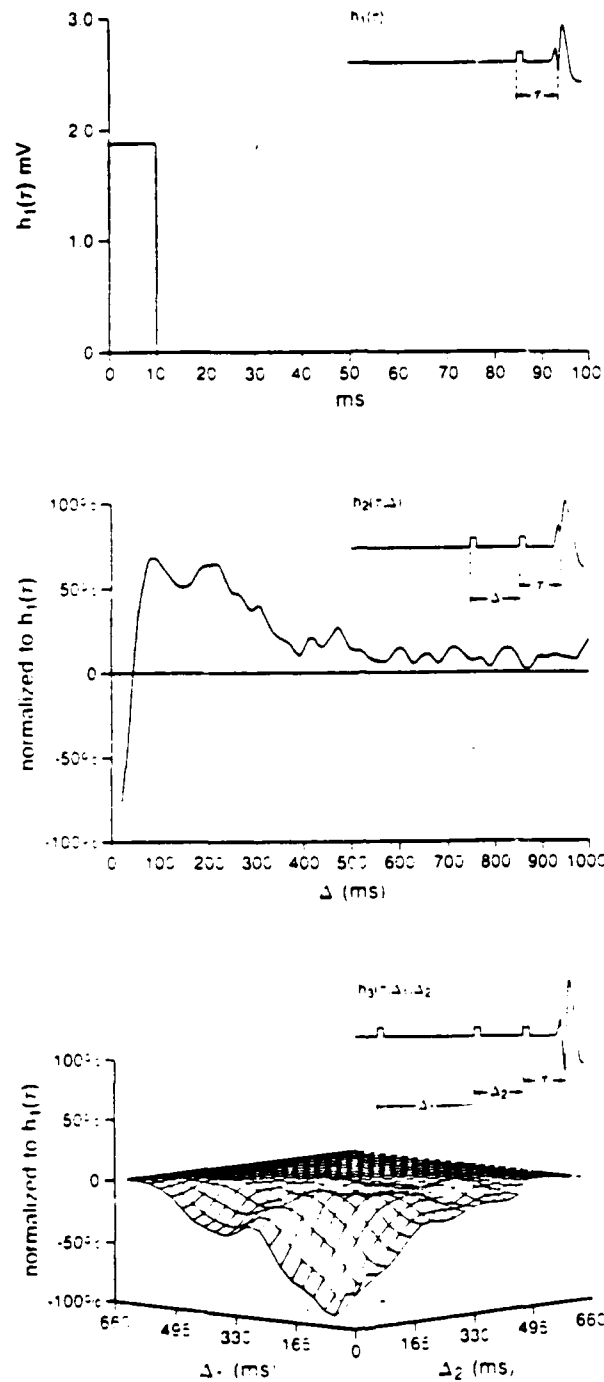


Figure 1: First, second, and third order kernels computed for dentate granule cell population spikes recorded in response to random impulse train stimulation of the perforant path. The first order kernel is the average population spike amplitude to all impulses in the train occurring with a latency of τ (see schematic, insert). The second order kernel represents the dependence of population spike amplitude on the interval (Δ) since any previous impulse in the train (see schematic, insert). The third order kernel represents the dependence of the population spike amplitude on the two intervals (Δ_1 , Δ_2) since any two previous impulses in the train not predicted by the first and second order kernels (see schematic, insert).

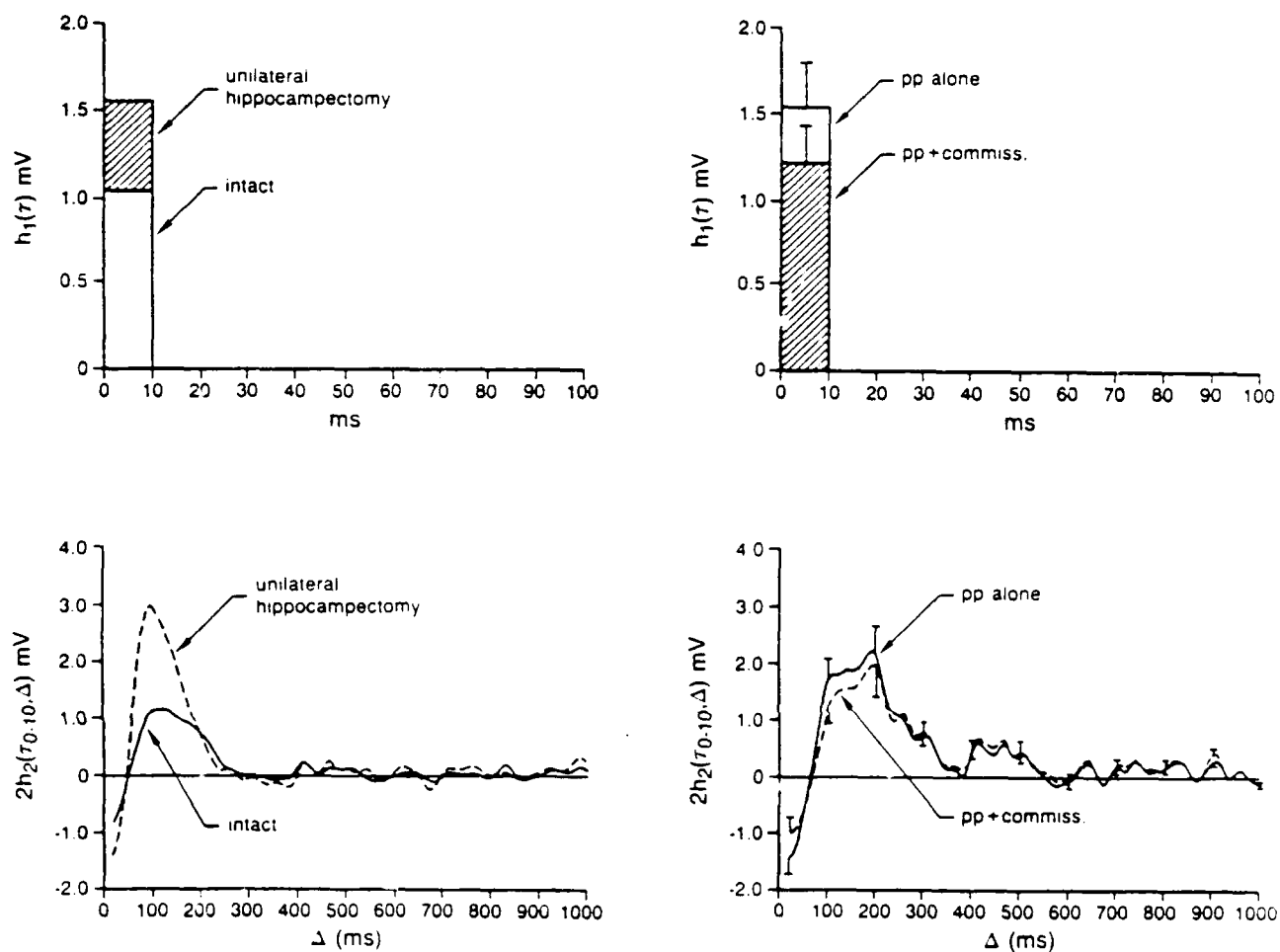


Figure 2: Effects of removing commissural feedback (left panel) or electrically stimulating commissural afferents (right panel) on first and second order kernels for granule cell responses to random train stimulation of medial perforant path. Note the opposite effects of the two manipulations

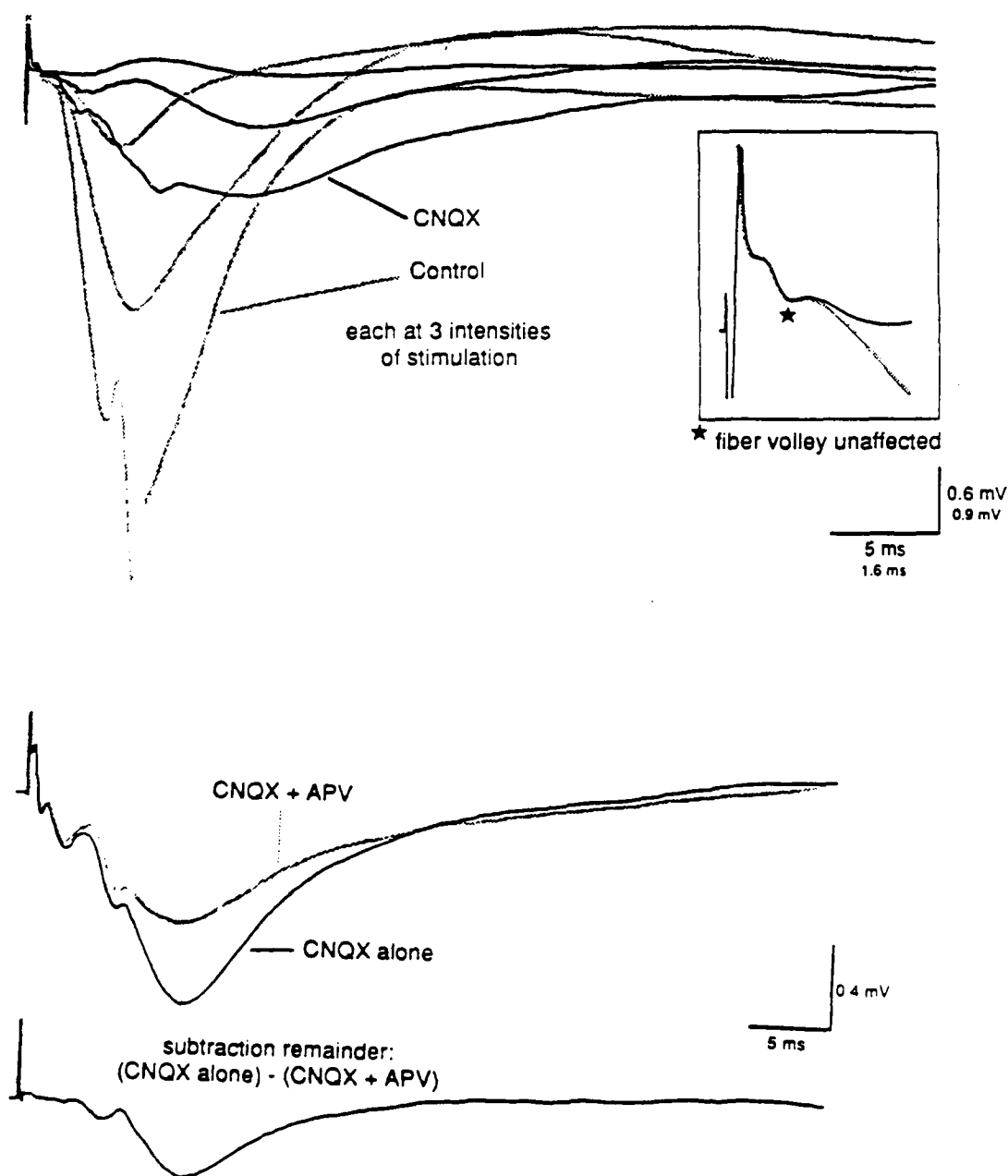


Figure 3. Demonstration of an NMDA receptor-mediated component of the granule cell population EPSP in the presence of CNQX. *Upper.* Responses evoked before and during application of CNQX using three stimulation intensities indicate that CNQX does not eliminate the response. *Lower.* Concurrent application of APV reduces the response which remains in the presence of CNQX. The NMDA receptor-mediated component of the response is calculated by subtracting the response in the presence of APV from that prior to its application.

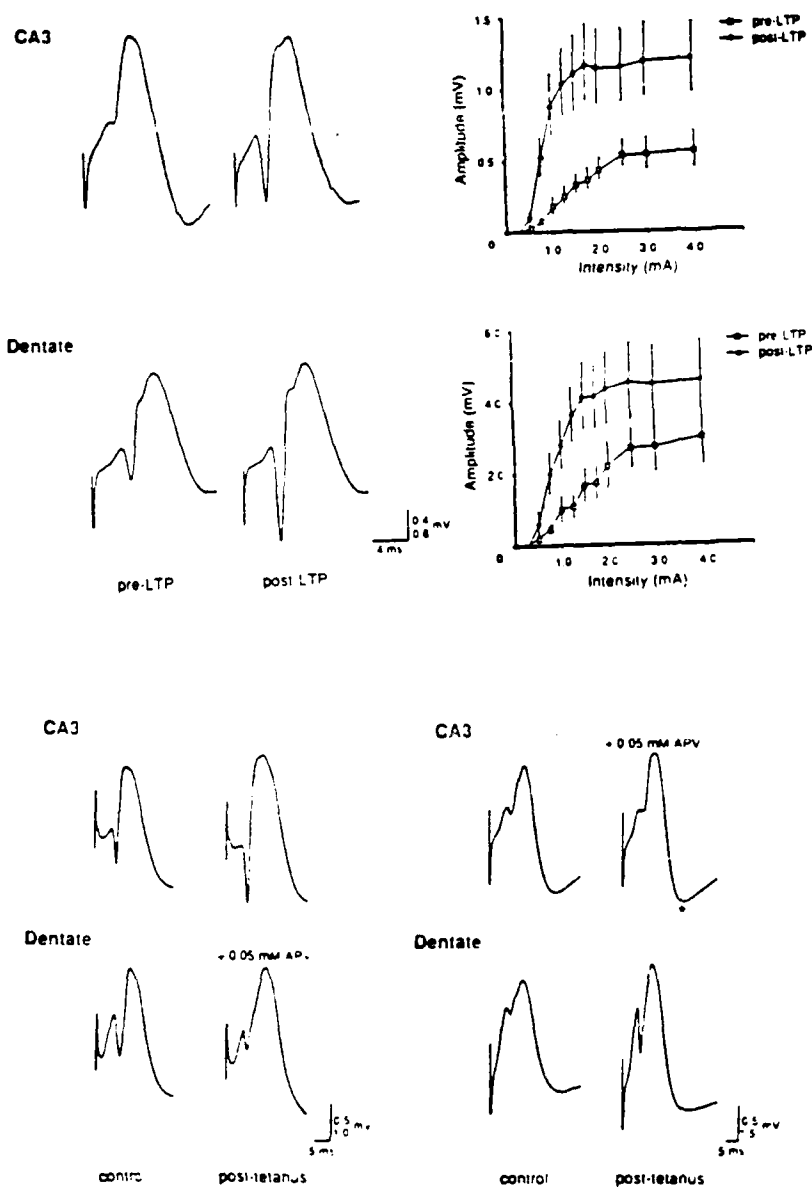


Figure 4: Top: Long-term potentiation of CA3 pyramidal cells and granule cells of the dentate gyrus by entorhinal afferents. (left) Averages of five responses simultaneously recorded from CA3 and the dentate gyrus before and 30 min. after the induction of perforant path LTP. (right) Summary of input/output graphs for ten animals in which LTP was induced. Bottom: Selective blockade of induction of perforant path LTP. Focal injection of the NMDA antagonist d-APV reversibly blocked perforant path LTP. (right) APV-sensitive blockade of LTP in CA3. The asterisk reflects an increase in disynaptic input from the selectively potentiated granule cells. All waveforms are averages of five responses.

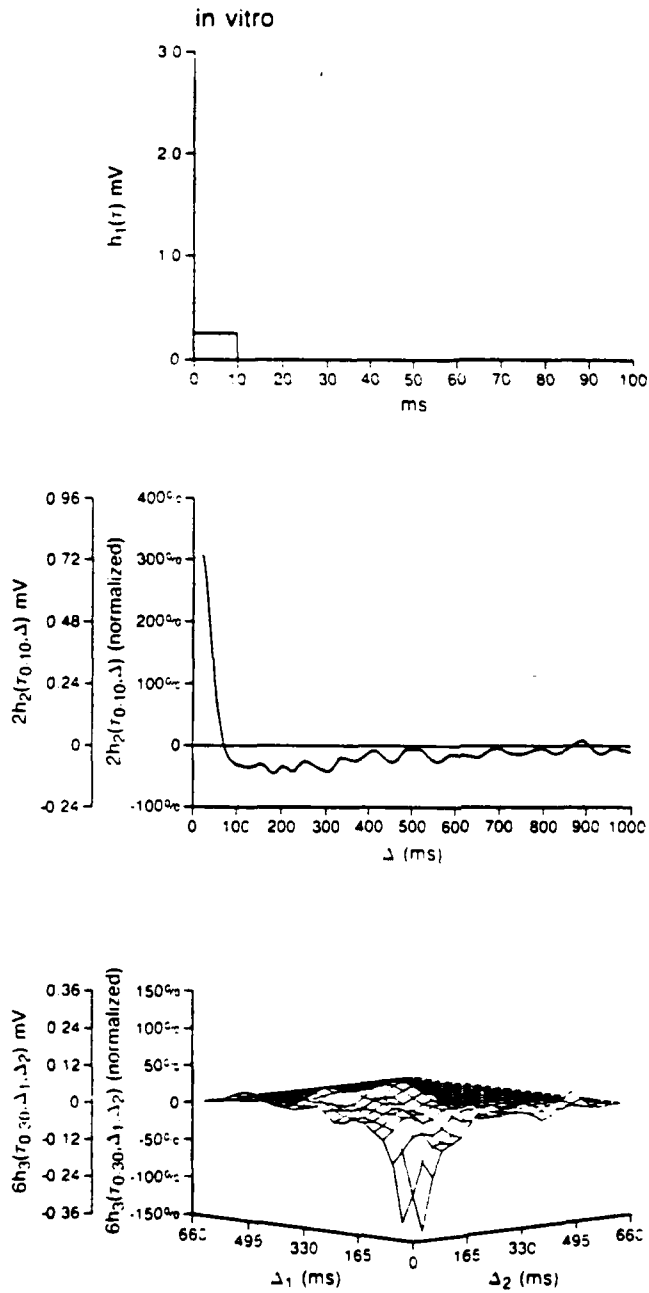


Figure 5: First (top), second (middle), and third (bottom) order kernels for granule cell responses to random train stimulation of medial perforant path using an *in vitro* slice preparation.

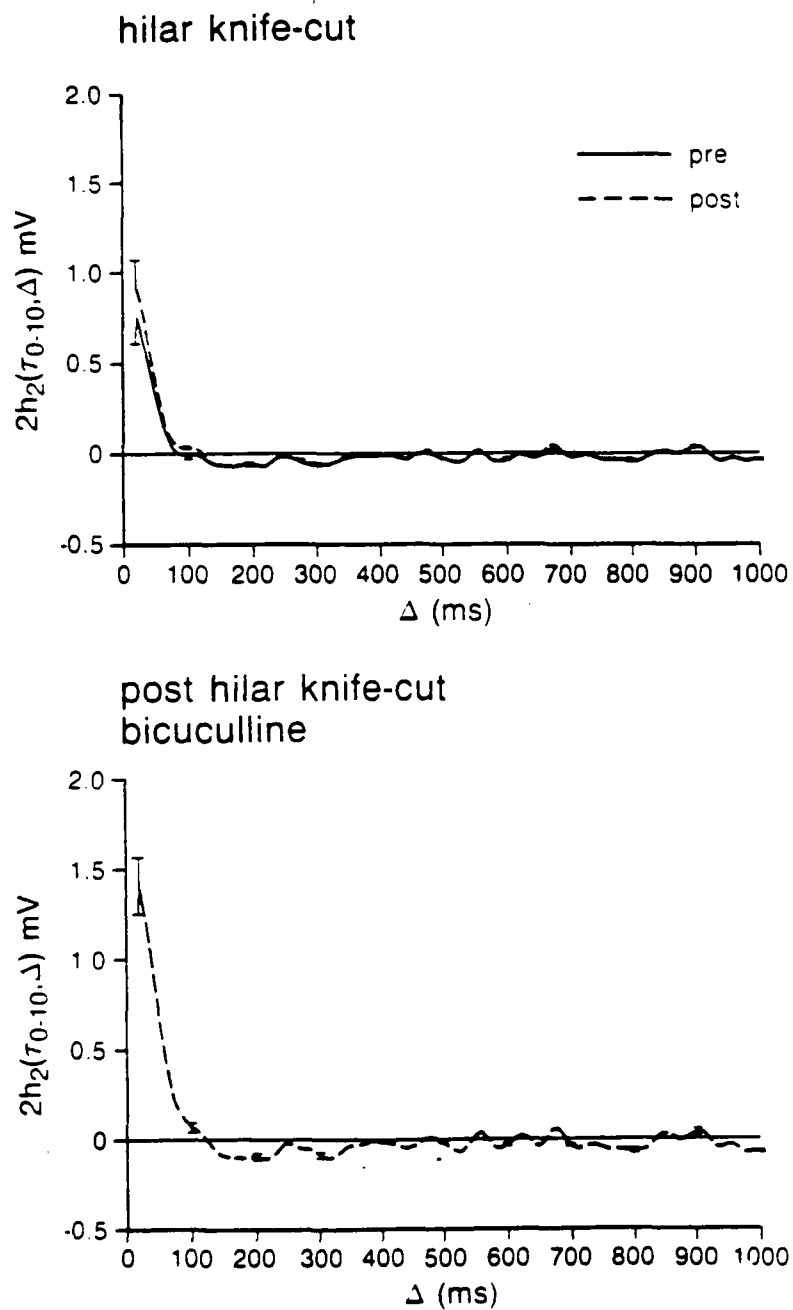


Figure 6: Top: Second order kernels before (solid) and after (dashed) surgically isolating the outer blade of the dentate gyrus from an *in vitro* hippocampal slice. Bottom: Effects of bicuculline on second order nonlinearities of the "mini" dentate slice.

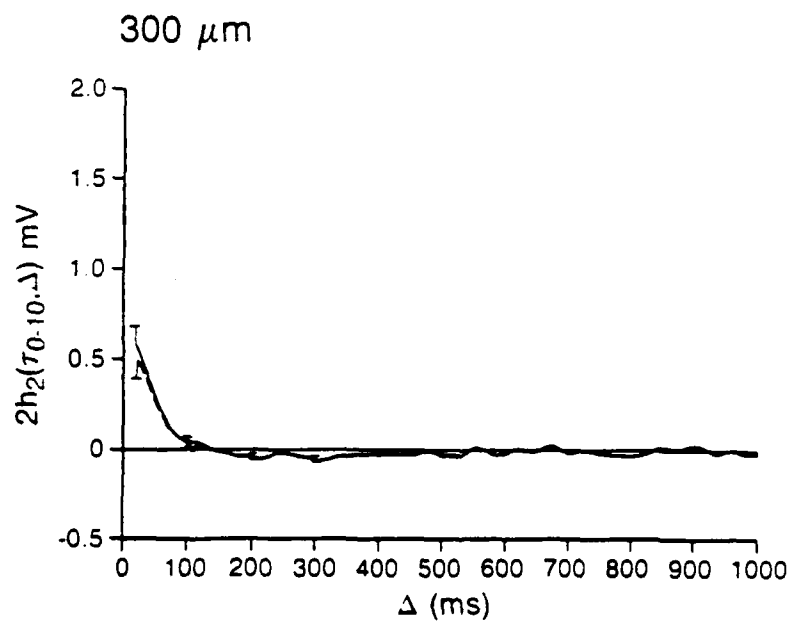
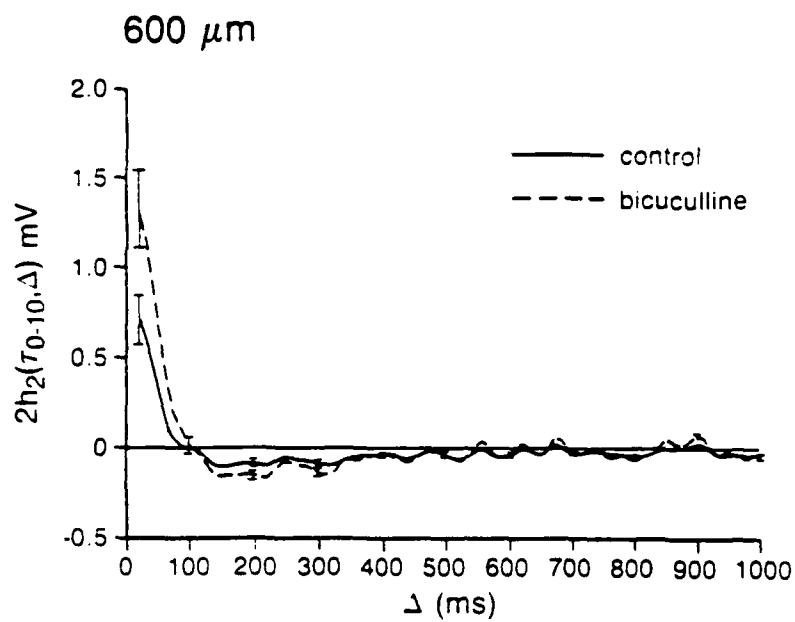


Figure 7: Effects of bicuculline on second order nonlinearities of dentate granule cells of a 600 μm and a 300 μm hippocampal slice.

Intracellular: Granule Cell

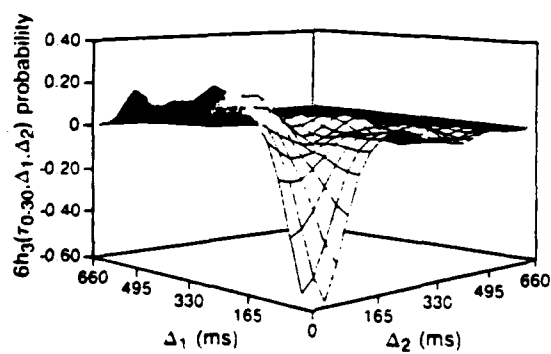
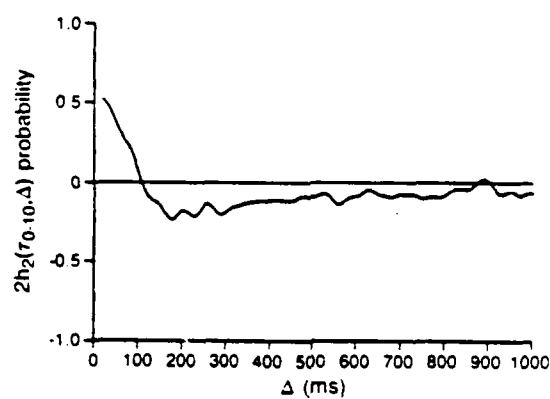
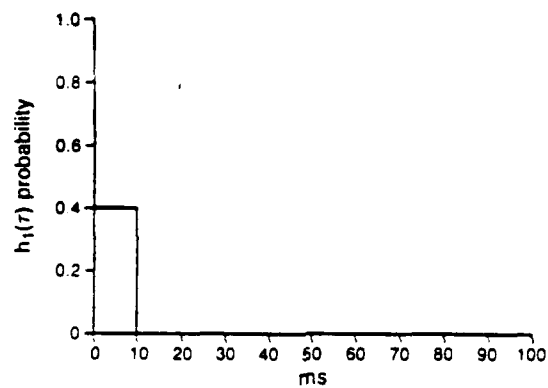


Figure 8: First (top), second (middle), and third (bottom) order kernels for an intracellularly recorded granule cell.

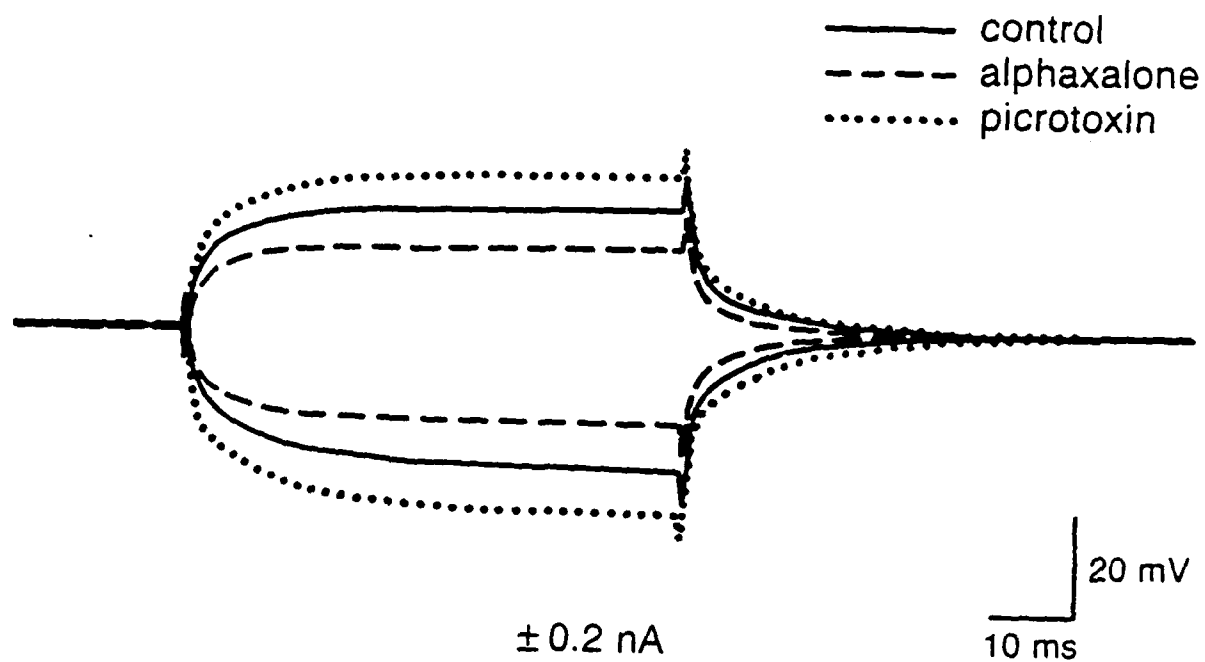


Figure 9: Effects of alphaxalone and picrotoxin on input resistance of a dentate granule cell *in vitro*.

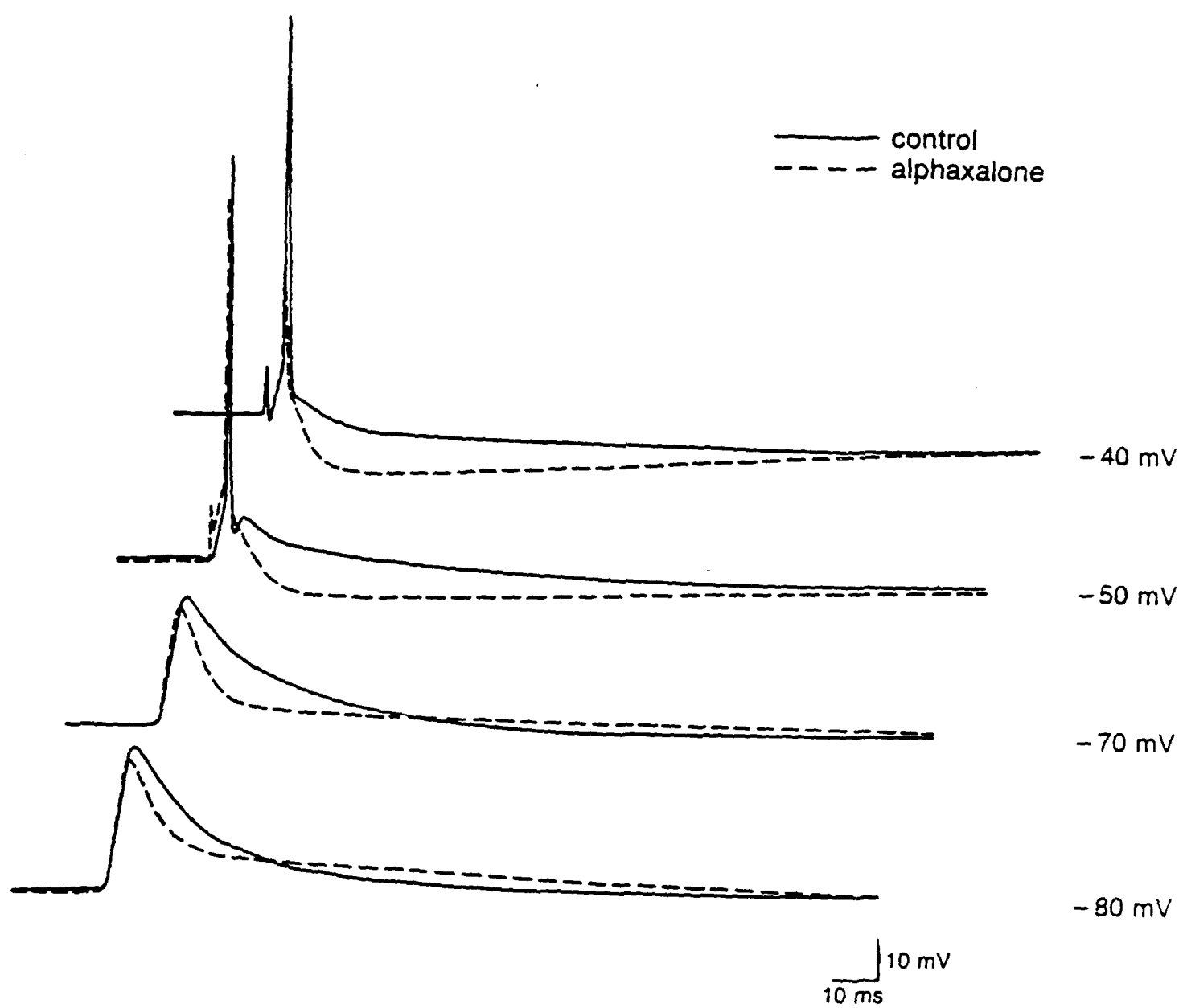


Figure 10: Effects of alphaxalone on orthodromically activated IPSPs recorded intracellularly from a dentate granule cell.

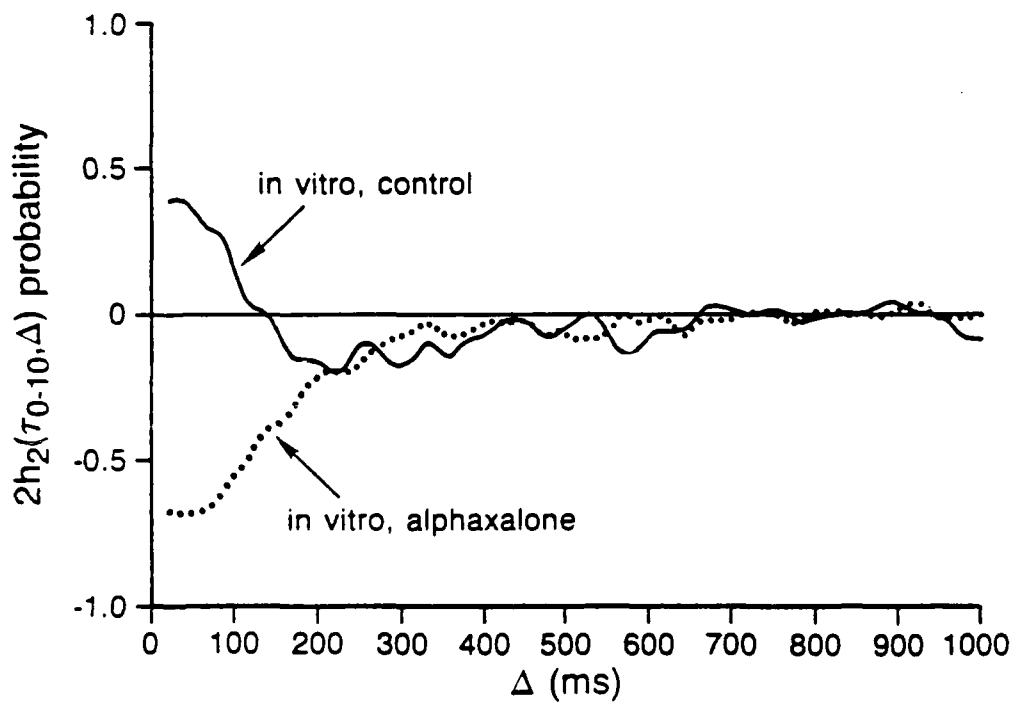


Figure 11: Effects of alfaxalone on second order nonlinearities of an intracellularly recorded granule cell.